Fish and Shellfish Immunology Reports 5 (2023) 100109

Contents lists available at ScienceDirect

Fish and Shellfish Immunology Reports

journal homepage: www.sciencedirect.com/journal/fish-and-shellfish-immunology-reports

The histidine phosphatase LHPP of *Penaeus vannamei* is involved in shrimp hemocytes apoptosis

Zhongyan Wang [a], Yueling Zhang [a,b], Jude Juventus Aweya [a], Zhongyang Lin [a], Defu Yao [a,*], Zhihong Zheng [a,*]

[a] Institute of Marine Sciences and Guangdong Provincial Key Laboratory of Marine Biotechnology, Shantou University, Shantou 515063, China
[b] STU-UMT Joint Shellfish Research Laboratory, Shantou University, Shantou 515063, China

ARTICLE INFO

Keywords:
Pvlhpp
Vibrio parahaemolyticus
Hemocyte
Apoptosis

ABSTRACT

LHPP (Phospholysine Phosphohistidine Inorganic Pyrophosphate Phosphatase) is a protein histidine phosphatase that modulates a hidden posttranslational modification called histidine phosphorylation. LHPP also acts as a tumor suppressor, which plays a pivotal role in various cellular processes. However, whether LHPP participates in the regulation of invertebrate's immunity is still unknown. Here we characterized a LHPP homolog in *P. vannamei* (designated *Pv*LHPP), with a 807 bp length of open reading frame (ORF) encoding a putative protein of 268 amino acids. Sequence analysis revealed that *Pv*LHPP contains a typical hydrolase 6 and hydrolase-like domain, which was conserved from invertebrate to vertebrate. *Pv*LHPP was ubiquitously expressed in tissues and induced in hemocyte and hepatopancreas by *Vibrio parahaemolyticus, Streptococcus iniae* and white spot syndrome virus (WSSV) challenge, indicating that *Pv*LHPP participated in the immune responses. Moreover, silencing of *Pv*LHPP followed by *V. parahaemolyticus* inhibited hemocyte apoptosis. This study enriches our current insight on shrimp immunity, and provides novel perspective to understand immune-regulatory role of *Pv*LHPP.

1. Introduction

Protein phosphorylation is normally modified at serine, threonine and tyrosine amino acid residues of protein in ukaryotes, which can directly regulate the stability, interaction, localization and enzymatic activity of target proteins by rapid and reversible modifications [1]. Histidine phosphorylation (pHis) is a poorly characterized phosphorylation, which is evolutionarily conserved from worm to human and plays crucial roles in signal transduction and cell metabolism. The pHis of protein has broader roles in cellular function including cell cycle regulation, phagocytosis, regulation of ion channel activity and metal ion coordination, which is reversible by specific kinases and phosphatases [2].

Phosphotyrosine phosphohistidine inorganic pyrophosphate phosphatase (LHPP) is an unique histidine phosphatase that contains a member of the haloacid dehalogenase (HAD) superfamily of hydrolases and eliminate histidine phosphorylation by dephosphorylating the phosphorylated active-site histidine [3]. Evidences support that LHPP mediated histidine dephosphorylation is play a pivotal role with various human diseases like tumorigenesis [4], major depressive disorder [5], alcohol dependence [6] and risky behavior [7]. Recent findings have provided new insights into how LHPP regulate cellular process. For example, LHPP suppressed cell proliferation and cell invasion of intrahepatic cholangiocarcinoma by decreasing SMAD phosphorylation and inhibit the transforming growth factor-beta (TGF-β) signaling [8]. Similarly, knockdown of LHPP promoted the proliferation and growth in bladder cancer cell, which inactivate AKT/p65-Bcl-2/Cyclin D1 signaling pathway by enhancing phosphorylation of AKT and p65 [9]. In addition, LHPP was downregulated in oral squamous cell carcinoma (OSCC) tissues, which promotes the apoptosis of OSCC by decreasing the transcriptional activity of p-PI3K and p-Akt [10]. In patients with hepatocellular carcinoma (HCC), loss of LHPP expression is associated with increased tumor severity and reduced patient survival [4]. Overexpression of LHPP can significantly reduce the proliferation and metastasis of cervical cancer cells and induce significant apoptosis of cervical cancer cells [11].

Although the role of pHis mediated by LHPP has been widely reported in vertebrates, the significance of invertebrate histidine

* Corresponding author.
E-mail addresses: dfyao@stu.edu.cn (D. Yao), zhengzh@stu.edu.cn (Z. Zheng).

https://doi.org/10.1016/j.fsirep.2023.100109
Received 4 December 2022; Received in revised form 11 June 2023; Accepted 26 June 2023
Available online 26 June 2023

Table 1
Primers and dsRNA sequences used in this article.

Primers name	Sequence (5′–3′)	Amplicon size (bp)
For gene expression		
*Pv*LHPP-F	CGCGGATCCATGAGCAACTGGCTGGAG	807
*Pv*LHPP-R	TCCCCCGGGTTATTTCTTATGAGCCTCTATAAT	807
Real-time RT-PCR		
*Pv*LHPP-qF	TGGATACAAAGTGAGCGAAGCA	159
*Pv*LHPP-qR	CCCATGACAACACATGATGGAC	
*Pv*EF-1α-F	TATGCTCCTTTTGGACGTTTTGC	118
*Pv*EF-1α-R	CCTTTTCTGCGGCCTTGGTAG	
dsRNA		
ds*Pv*LHPP F	TATCTTTAGCCCTGTGCCAGC	403
ds*Pv*LHPP R	TCCCACCATCACCACCTCTT	
ds*Pv*LHPP T7F	GGATCCTAATACGACTCACTATAGGTATCTTTAGCCCTGTGCCAGC	
ds*Pv*LHPP T7R	GGATCCTAATACGACTCACTATAGGTCCCACCATCACCACCTCTT	

phosphorylation has rarely discovered in some aquatic invertebrates like shrimp, which is an economic aquatic arthropod and act as a unique role in evolution of animal immunity. Interestingly, our in-lab transcriptome data revealed that expression of phosphohistidine inorganic pyrophosphate phosphatase (LHPP) was up-regulated in shrimp after LPS stimulation [12], which suggest that LHPP may play pivotal role in the immune system of shrimp. In the current study, a full-length of LHPP ORF from *P. vannamei* (*Pv*LHPP) was cloned and its spatial and temporal expression profiles were investigated to illustrate its role in response to *V. parahaemolyticus* challenge. We also confirmed the pro-apoptosis effect of *Pv*LHPP by RNA interference. This study provides new insights for understanding the role of LHPP in innate immunity of invertebrates.

2. Materials and methods

2.1. Experimental shrimp and sample collection

Pacific white shrimp (*P. vannamei*) approximately 8 g each and irrespective of sex, were obtained from a local shrimp farm, Shantou Huaxun Aquatic Product Corporation Farm (Shantou, Guangdong, China). All shrimp were acclimated in water at 23 ± 2 °C, 10 g/L salinity, and sufficient aeration for three days before used for the experiment. Five healthy shrimp were randomly selected from each group and hemolymph was extracted directly from pericardial sinus with 1.0 mL disposable sterile syringe and needle into an equal volume of precooled acid citrate dextrose (ACD) anti-coagulant buffer (19.65 g/L NaCl, 22.8 g/L glucose, 7.95 g/L sodium citrate, and 3.35 g/L EDTA-Na2, pH 6.0). Then hemocytes were collected by centrifugation at 800 g for 10 min at 4 °C for immediate use. Other shrimp tissues such as hepatopancreas, heart, gill, muscle, eyestalk, stomach, nerve, and intestine were excised and ground immediately to pulverize in liquid nitrogen for RNA extraction. All animal experiments were carried out with guidelines and approval of the Animal Research and Ethics Committees of Shantou University, China.

2.2. Total RNA extraction and cDNA synthesis

Total RNA was extracted from various shrimp tissues (hemocytes, hepatopancreas, gill, intestine, eyestalk, heart, muscle, nerve and stomach) using the RNAFAST 200 kit (FeiJie, Shanghai, China) according to the manufacturer's instruction. The RNA concentration was quantified by NanoDrop 2000 spectrophotometer (Nano-drop Technologies, Wilmington, DE), while RNA quality was evaluated by 1% agarose gel electrophoresis. Then, total RNA was reverse transcribed into cDNA using a commercial kit (TransGen Biotech, Beijing, China) and used for real-time quantitative polymerase chain reaction (qPCR) analysis.

2.3. Sequence and bioinformatics analysis

Full-length cDNA sequence encoded putative *Pv*LHPP protein was retrieved from our in-house *P. vannamei* transcriptome data. The open reading frame (ORF) of *Pv*LHPP was predicted using ORF finder (http://www.ncbi.nlm.nih.gov/gorf/gorf.html). Gene specific primers (designed by Primer premier 5 software) targeting to the ORF of *Pv*LHPP (Table 1) were used for gene amplification by PCR. PCR products were cloned into the pMD-19T vector (Takara, Japan) and sequenced using Sanger sequencing technology at Beijing Genomics Institute (BGI, Shenzhen, China). EXPASY (Expert Protein Analysis System, http://www.expasy.org) was used to translate *Pv*LHPP nucleotide sequence into amino acid sequence, then simple modular architecture research tool (SMART) (http://smart.embl-heidelberg.de) was employed to predict the functional domains of *Pv*LHPP and LHPP from other species. BLAST program (http://www.ncbi.nlm.nih.gov/BLAST/) was utilized to find regions of similarity of *Pv*LHPP nucleotide sequences against other species, while the phylogenic tree (neighbor-joining) was constructed based on the full-length amino acid sequences of LHPP orthologous sequences of *P. vannamei* and other species by using the MEGA 7.0 software (bootstrapped for 1000 times).

2.4. Tissue distribution of PvLHPP transcript

The expression of *Pv*LHPP in different tissues (i.e., shrimp hemocytes, hepatopancreas, gill, intestine, eyestalk, heart, muscle, nerve and stomach) was determined by Realtime quantitative polymerase chain reaction (qPCR). Gene-specific primers were designed (Table 1) based on the partial ORF of *Pv*LHPP and elongation factor 1 alpha gene of *P. vannamei* (*Pv*EF1 α), which was used as internal control. The qPCR reaction was carried out using Master SYBR Green I system (GenStar, Beijing, China) on LightCycler 480 (Roche, Switzerland) with the following cycling conditions: one cycle at 95 °C for 10 min and 45 cycles of 95 °C for 15 s and 60 °C for 30 s. The expression of *Pv*LHPP was calculated by the $2^{-\triangle\triangle CT}$ method [13] relative to the internal control (*Pv*EF-1α). The expression levels of the other tissues were normalized to the tissue with the lowest expression. All samples were analyzed in triplicates.

2.5. Immune challenge

For pathogen challenge experiments, three hundred healthy shrimp were randomly divided into four groups (75 individuals/group). *V. parahaemolyticus* and *S. iniae* were inoculated into thiosulfate-citrate-bile salts-sucrose (TSB) and Luria-Bertani (LB) medium respectively and cultured in a shaker at 37 °C. WSSV was purified from infected crayfish *Procambarus clarkii* using differential centrifugation and quantified by spectrophotometry as previously described [14,15]. Each shrimp was intramuscularly injected with 100 μL pathogen or PBS (pH 7.4, 0.01 M) at the third abdominal segment. For the challenge group, *V. parahaemolyticus* (5×10^5 CFU/shrimp), *S. iniae* (1×10^6 CFU/shrimp), and WSSV (1×10^4 virus copies/shrimp) were injected respectively, while the control group was injected with PBS. At 0, 6, 12, 24, 48

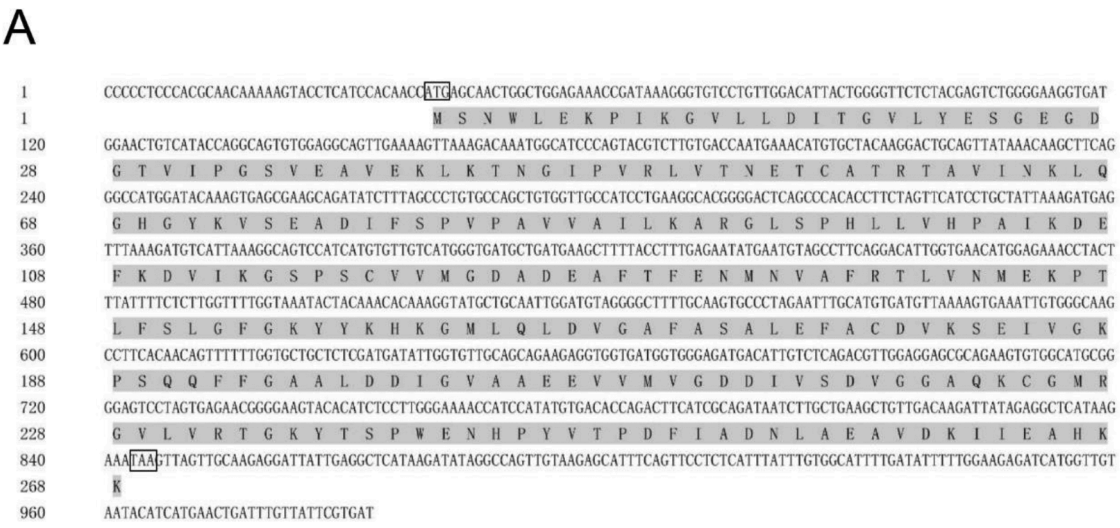

Fig. 1. Nucleotide sequence of *P. vannamei* LHPP with deduced amino acid sequence and structural domain. (A) The ORF of amino acid sequences are shown with one-letter codon. Nucleotides and amino acids are numbered on the left of sequences. Initiation codon (ATG) and stop codon (TAA) are enclosed. (B) The predicted functional domain of LHPP protein in different species. (C) Multiple sequence alignment between *Pv*LHPP and LHPP proteins from other species including *Drosophila hydei* (XP_023170253.1), *Homo sapiens* (AAI13630.1), *Numida meleagris* (XP_021255183.1), *Danio rerio* (NP_001092251.1) and *Xenopus laevis* (AAI06525.1). Identical amino acid residues are shaded in black, 75% of similar amino acid residues are dark gray, and 50% of similar amino acid residues are light gray. (D) The neighbor-joining phylogenetic tree based on the sequences of LHPP proteins from *Astatotilapia calliptera* LHPP (XP_026034240.1), *Oreochromis niloticus* LHPP (XP_025765458.1), *Mastacembelus armatus* LHPP (XP_026170537.1), *Monopterus albus* (XP_020460847.1), *Electrophorus electricus* LHPP (XP_026872591.2), *Danio rerio* LHPP (NP_001092251.1), *Pseudonaja textilis* LHPP (XP_026560719.1), *Zonotrichia albicollis* LHPP (XP_014125235.2), *Xiphorhynchus elegans* (NXU88692.1), *Homo sapiens* LHPP (AAI13630.1), *Desmodus rotundus* LHPP (XP_024411257.1), *Exaiptasia diaphana* (KXJ15712.1), *Strongylocentrotus purpuratus LHPP* (XP_030841317.1), *Hirondellea gigas* LHPP (LAB69461.1), *Drosophila hydei* LHPP (XP_023170253.1). Numbers marked on the tree branches represent bootstrap values. Location of *Pv*LHPP is indicated by a black filled triangle.

and 72 h post-injection (hpi) of pathogen or PBS, hemocytes and hepatopancreas samples were collected from 2 shrimp per group. Total RNA was extracted and cDNA was synthesized, then the transcript level of *Pv*LHPP was determined by qPCR. All samples were prepared in triplicate and data were expressed as mean ± standard error.

2.6. RNA interference (RNAi) of PvLHPP

The dsRNA-specific primers (Table 1) of the *Pv*LHPP gene were designed with Primer Premier 5 software. Double-strand RNA (dsRNA) was used for RNA interference (RNAi) experiment, *Pv*LHPP dsRNA

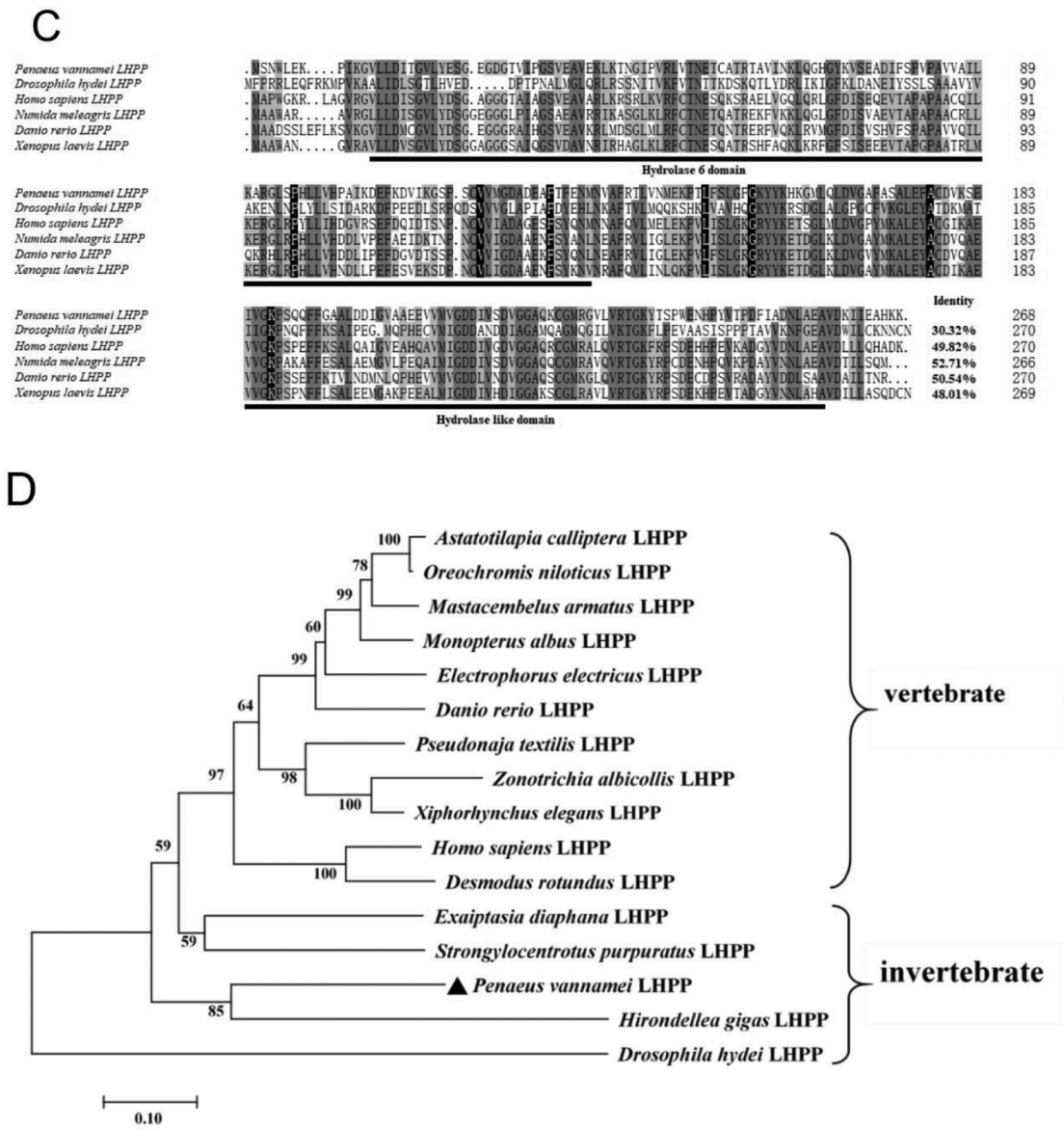

Fig. 1. (*continued*).

(ds*Pv*LHPP) and enhanced green fluorescent protein dsRNA (dsEGFP) were obtained by in vitro transcription using T7 RiboMAX™ Express RNAi System (Promega, USA). For RNAi assay, 100 μL of 5.0 μg of ds*Pv*LHPP or dsEGFP were respectively introduced into shrimp twice with an interval of 24 h by intramuscular injection. Shrimp hemocytes were collected from experiment group and control group at 48, 72 and 96 hpi, three shrimps were sampled from each group at each time point, followed by RNA extraction, cDNA synthesis and qPCR analysis to determine the knockdown efficiency of *Pv*LHPP. Relative expression of *Pv*LHPP was detected with gene-specific primers (Table 1). All samples were prepared in triplicate and data were expressed as mean ± standard error.

2.7. Extraction of total protein of hemocyte

Hemocyte mixed samples of six shrimps from each treatment group were used to prepare total hemocyte protein for Western blot. Hemolymph was extracted from shrimp with 1 mL sterile syringe, and mixed with 1:1 anticoagulant, centrifuged at 1000 g at 4 °C for 10 min, and cell precipitation was obtained. After washing the cells with PBS three times, 100 μL cell lysis buffer (RIPA lysis buffer) containing 1 μL protease inhibitor cocktail (EDTA-free, 100 ×) and 1 μL PMSF (100 ×) was added and lysed on ice for 10 min. The cell lysate was centrifuged at 20, 000 g at 4 °C for 20 min, and the supernatant was mixed with 5 × SDS loading buffer and heated at 100 °C for 10 min. The samples were stored at −40 °C before used.

2.8. SDS-PAGE and Western blotting

Protein samples were separated with SDS-PAGE and transferred onto poly-vinylidene fluoride (*PV*DF) membrane (Millipore, Billerica, MA, USA) using Mini Trans-Blot® Electrophoretic Transfer Cell Instruction (Bio-Rad, Richmond, CA, USA). Then *PV*DF membrane was blocked for 2 h at room temperature with 5% skimmed milk dissolved in Tris buffer solution with Tween (TBST) (20 mM Tris, 150 mM NaCl, 0.1% Tween 20, pH 7.4). The membranes were incubated overnight at 4 °C with rabbit anti-human Caspase 3 antibody (1:1000, Abcam, batch ab93680, Cambridge, UK), rabbit anti-human Caspase 9 antibody (1: 1000, Abcam, batch ab93680, Cambridge, UK), rabbit anti-human Bax antibody (1:1000, Abcam, batch ab93680, Cambridge, UK) or mouse anti-human Tubulin antibody (1: 3000, Sigma-Aldrich, St. Louis, MO, USA) respectively, followed by washing 3 times (10 min) with TBST. Then,

after incubation with the corresponding secondary antibody for 1 h at room temperature, the membranes were washed with TBST three times (10 min each). Immunoreactive bands are visualized by enhanced chemiluminescence (ECL) reagent (Millipore, Billerica, MA, USA) and detected on Amersham Imager 600 (GE, Boston, MA, USA).

2.9. Analysis of hemocytes apoptosis after PvLHPP knockdown

Sixty shrimp were randomly divided into two groups and injected intramuscularly with 5 μg dsEGFP or ds*Pv*LHPP respectively followed by challenging with *V. parahaemolyticus* (5×10^5 CFU/shrimp). Hemocytes were collected from 6 shrimp in each group at 4 hpi for flow cytometry analysis and Caspase 3/7 activity determination as described in previous study [16]. Firstly, YO-PRO™−1 dye/Propidium Iodide (PI) double staining kit (Thermo Fisher Scientific, Cleveland, OH, USA) was used for flow cytometry analysis according to manufacturer's instructions. In details, working solution with 20 μg/mL of YO-PRO-1 and 50 μg/mL PI were dissolved in anti-coagulant buffer and stored away from light on ice. Hemocytes were filtered through a flow cytometry tube, and a minimum of 6×10^5 hemocytes were re-suspended in 1 mL of working buffer and stained for 15 min at room temperature darkly. The collected events were recorded on a dot plot through fluorescence signal measurement and analysis with Accuri C6 flow cytometer (BD Bioscience, San Diego, USA). Secondly, the activity of Caspase 3/7 was assayed by Caspase-Glo® 3/7 assay kit (Promega, USA). Briefly, hemocytes were collected, and 30 μL hemocytes (6000 cells) and 30 μL reaction buffers were seeded into an opaque 96-well plate, which were gently mixed on the rocker and incubated at room temperature for 4 h. Caspase 3/7 activity was measured using a Multimode microplate reader (Infinite™ F200, Tecan, Switzerland). Three independent samples were tested each time, and each sample was analyzed three times.

2.10. Statistical analysis

All statistical analyses used GraphPad Prism Version 8.0.1 (GraphPad Software Inc., San Diego, CA, USA). Data are mainly presented as mean ± standard deviation (SD) unless otherwise stated. An unpaired two-tailed student's *t*-test or an one-way analysis of variance (one-way ANOVA) was used to determine the significant difference (considered at $p < 0.05$) between different groups where data was distributed normally with the equal variance between conditions.

3. Results

3.1. Cloning and sequence analysis of PvLHPP

The sequence of shrimp *Pv*LHPP was retrieved from *P. vannamei* transcriptome data which were submitted to GenBank with accession numbers PRJNA420111 [12]. After DNA sequencing and BLAST analysis, the cloned sequence was submitted to the NCBI database with accession number MW508885. The complete open reading frame (ORF) of *Pv*LHPP is 807 bp, encoding a putative protein of 268 amino acids (GenBank accession number XP_027224718.1) (Fig. 1A). With an online SMART program to predict functional domains, *Pv*LHPP contains a hydrolase 6 domain (amino acids 12–133) and a hydrolase-like domain (amino acids 184–258) (Fig. 1B), which shared 30.32% - 52.71% homology with LHPP of other species (Fig. 1C), suggesting that it belongs to the typical phosphatase and hydrolase family. Phylogenetic analysis based on amino acid sequence showed that *Pv*LHPP and *Hirondellea gigas* LHPP clustered together in invertebrate clade (Fig. 1D).

3.2. Tissue specific and pathogens inducible expression profiles of PvLHPP

Expression of *Pv*LHPP mRNA relative to *Pv*EF1α in different tissues of healthy shrimp, including hemocytes, hepatopancreas, muscle, gill, nerve, intestine, heart, stomach and eyestalk, were detected by qPCR.

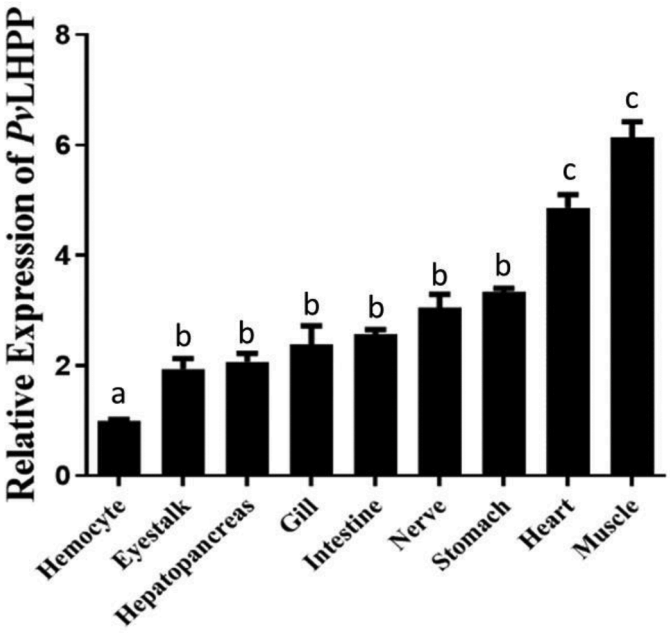

Fig. 2. Tissue distribution of *Pv*LHPP in healthy shrimp. The transcript level of *Pv*LHPP in different tissues (ie. hemocyte, eyestalk, hepatopancreas, gill, intestine, nerve, stomach, heart and muscle) were determined by qPCR with *Pv*EF1-α as the internal control. The mRNA level of *Pv*LHPP in hemocytes was set as 1.0 for which the others were normalized. Data represent mean ± SD ($n = 3$). Experiments were repeated at least three times and significance of difference was determined by one-way ANOVA. Significance between different tissues was considered at $p < 0.05$ and indicated by different letters (a, b and ab).

Results showed that *Pv*LHPP transcripts were ubiquitously expressed in all examined tissues. Among these tissues, transcripts of *Pv*LHPP were most abundance in muscle and heart, moderate in stomach, nerve, intestine, gill, hepatopancreas and eyestalk, and relative low expression in hemocyte (Fig. 2A). Since LHPP response to LPS challenge in shrimp hemocyte [12], several shrimp pathogens like *V. parahaemolyticus, S. iniae* and WSSV were used to challenge shrimp and the response of LHPP were detected in the major innate immune executors like hemocyte and hepatopancreas, which undertake an anti-infective immune response in shrimp. With *V. parahaemolyticus* challenge, relative expression of *Pv*LHPP in hemocytes was increased at 6, 24 and 48 hpi and sharply decreased at 36 h (Fig. 3A), while that in hepatopancreas increased rapidly and reach a peak at 36 and 48 hpi (Fig. 3B). In response to *S. iniae* challenge, *Pv*LHPP in hemocytes increased at 24 hpi and reached a peak at 36 hpi, then recovered to baseline later (Fig. 3C). Similarly, *Pv*LHPP expression in hepatopancreas increased at 6 hpi and reach a peak at 36 hpi, followed by recovering to baseline at 48 hpi (Fig. 3D). For WSSV treatment, *Pv*LHPP expression in hemocytes increased at 6, 24, 36 and 48 hpi (Fig. 3E), and expression of *Pv*LHPP in hepatopancreas increased sharply at 6, 24 and 36 hpi (Fig. 3F). In general, under stimulation of these pathogens, the transcription level of *Pv*LHPP is significantly induced in hemocytes and hepatopancreas of shrimp, especially in response to *V. parahaemolyticus* challenge, LHPP was continually changed in hemocyte (Fig. 3A). These results indicate that *Pv*LHPP has a strong and extensive response to pathogen challenge.

3.3. PvLHPP interference inhibits V. parahaemolyticus induced hemocytes apoptosis

To further explore the role of *Pv*LHPP in response to *V. parahaemolyticus* challenge, ds*Pv*LHPP targeting partial region of *Pv*LHPP ORF was designed and RNA interference was performed. The knockdown efficiency of *Pv*LHPP in hemocyte of shrimp was detected by

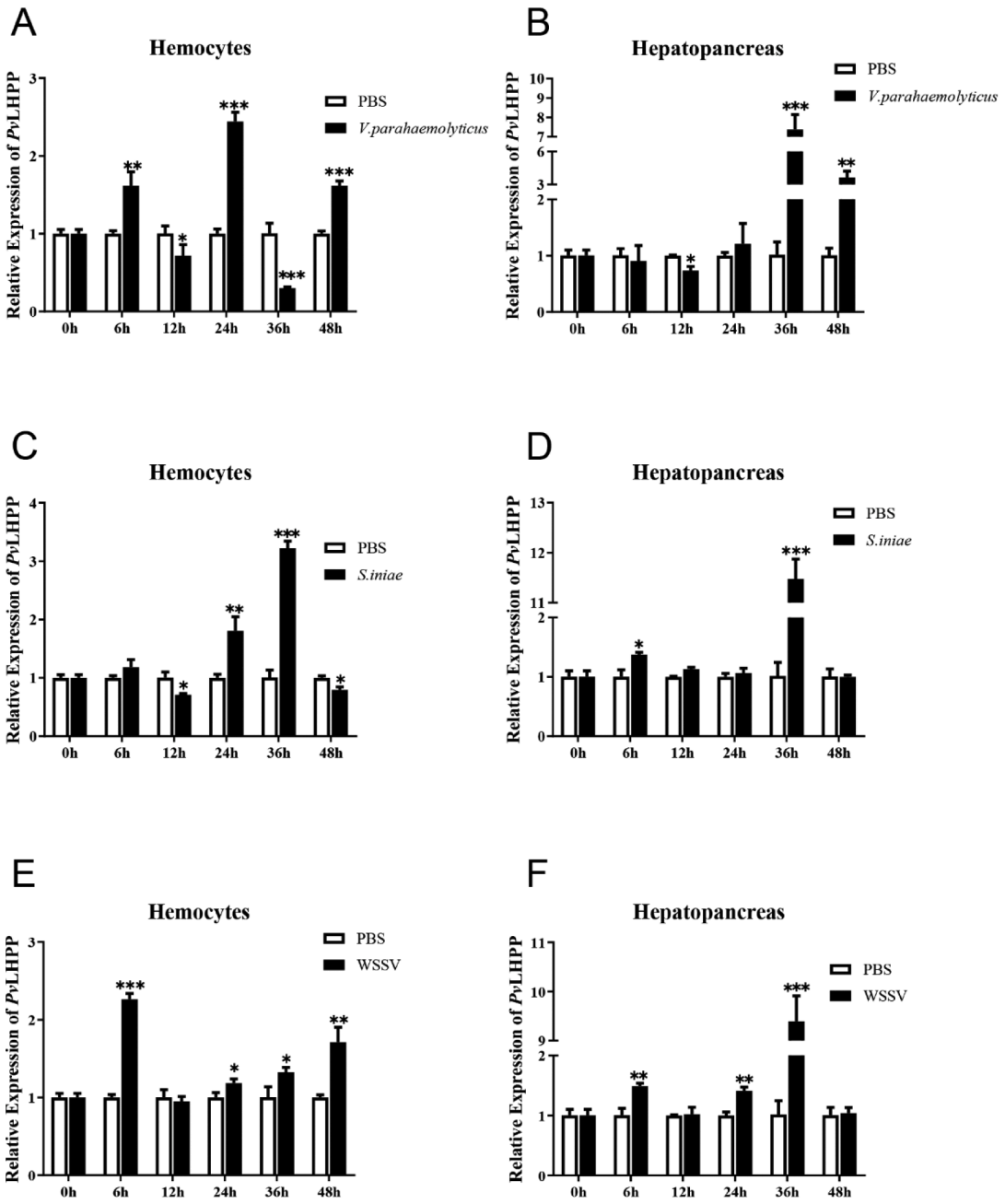

Fig. 3. Expression of *Pv*LHPP in hemocytes and hepatopancreas at 0–48 hpi with (A-B) *V. parahaemolyticus*, (C-D) *S. iniae* and WSSV (E-F) challenge. Expression of *Pv*LHPP was determined by real time qPCR analysis and relative to *Pv*EF1α expression. *Pv*LHPP expression level at 0 h of each group was set to 1.0. Experiments were repeated at least three times and significance of difference was determined by student's *t*-test relative to control and indicated by asterisks (*$p<0.05$, ** $p< 0.01$, *** $p< 0.001$).

qPCR. The result indicated that *Pv*LHPP was successfully knockdown with a decrease of 71.63% of transcript level ($p<0.01$) (Fig. 4A).

As a tumor suppressor, one of the major anti-tumor mechanisms of LHPP is to trigger tumor cell apoptosis [17], hence, the association of *Pv*LHPP and apoptosis in shrimp was further explored. After successfully knockdown of *Pv*LHPP by dsLHPP injection, a 4 hour of *V. parahaemolyticus* stimulation was carried out, then the apoptosis related indexes were detected in hemocyte. As shown in Fig. 4B, there was a significant decrease in the proapoptotic protein expression levels like caspase 3 and Bax in *Pv*LHPP depleted hemocyte, and a downtrend in the proapoptotic protein expression levels like caspase 9 in *Pv*LHPP depleted hemocyte. Besides, the decrease of *Pv*LHPP also reduced the mRNA expression of some proapoptotic genes like cytochrome C ($p<0.001$), P53 ($p<0.05$), caspase 3 ($p<0.001$) and Bax ($p<0.001$) (Fig. 4C). Given that *Pv*LHPP depletion reduced some proapoptotic genes and proteins in hemocyte, we determined whether hemocyte apoptosis occurred in *Pv*LHPP depleted shrimp upon *V. parahaemolyticus* challenge. The result showed that *V. parahaemolyticus* induced a significant decrease of Caspase 3/7 activity in *Pv*LHPP depleted hemocyte compared with control group, while silencing of *Pv*LHPP alone caused no significant change in the level of Caspase 3/7 activity (Fig. 4D). Moreover, flow cytometry analysis with Annexin V/propidium iodide staining revealed that knockdown of *Pv*LHPP decreased the percentage of apoptotic hemocyte under *V. parahaemolyticus* stimulation (Fig. 4E). These results indicate that *Pv*LHPP presented pro-apoptosis effect in shrimp hemocyte with *V. parahaemolyticus* infection.

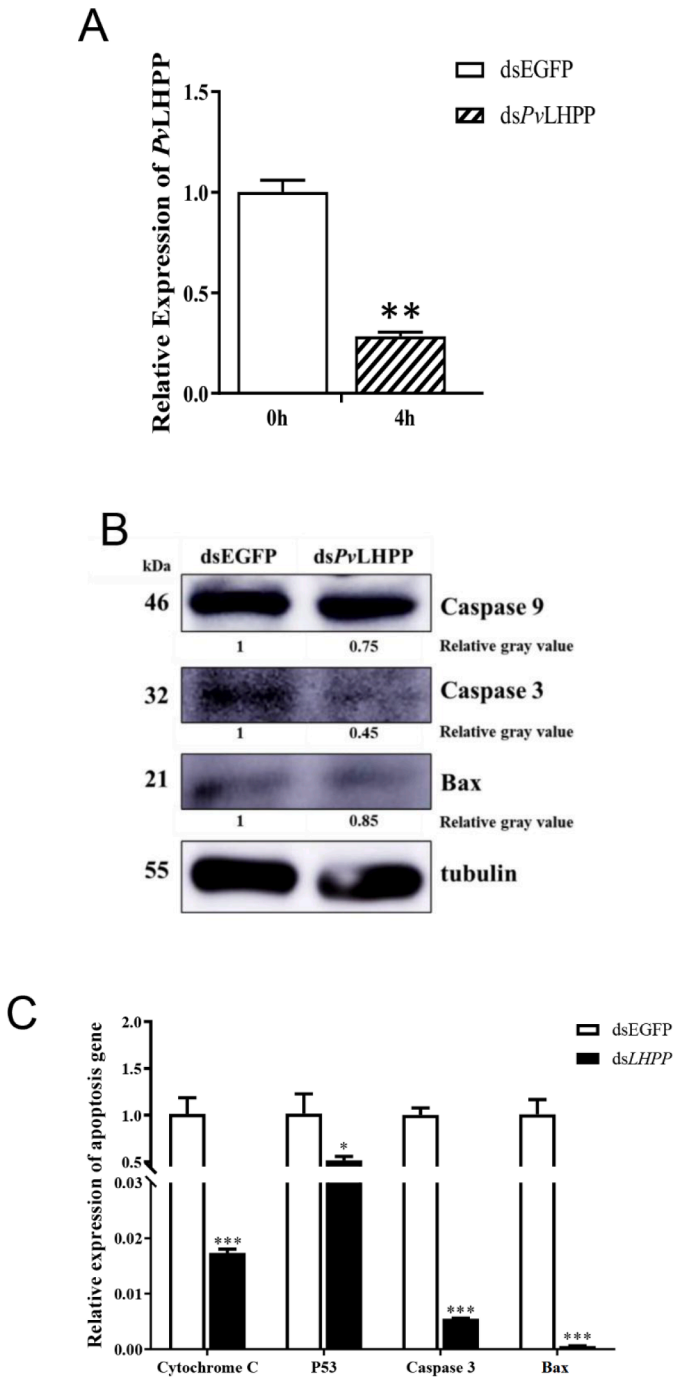

Fig. 4. Apoptosis of hemocytes after *Pv*LHPP knockdown in *P. vannamei* was analyzed by flow cytometry. (A) Shrimp were injected with dsEGFP and ds*Pv*LHPP for 72 h and followed by challenging with *V. parahaemolyticus for* 4 h. Hemocyte were collected and the knockdown efficiency was measured by qPCR. The transcripts of *Pv*LHPP in dsEGFP injected groups was set to 1.0 for which the others were normalized. (B) Caspase 9, caspase 3 and Bax protein levels in dsEGFP and ds*Pv*LHPP group were analyzed by Western blot. Cell lysates were analyzed using the appropriate antibodies, with tubulin used as an internal control. Numbers below the blots represent the relative gray values determined using ImageJ software. (C) Flow cytometric analysis of apoptosis was performed in *P. vannamei* hemocyte from dsEGFP and ds*Pv*LHPP group with *V. parahaemolyticus* challenge, hemocytes were stained with YO-PRO™−1 dye/Propidium Iodide double staining kit. Quadrants: lower-left represent live cells (YO-PRO™−1 negative/PI negative); lower-right represent early apoptotic/primary apoptotic cells (YO-PRO™−1 positive/PI negative); upper-right represent late apoptotic/secondary apoptotic cells (YO-PRO™−1 positive/PI positive); upper-left represent necrotic cells (YO-PRO™−1 negative/PI positive). The percentage of apoptotic cells were quantified and presented on the right. Data represent mean ± SD ($n = 3$). Asterisks represent statistically significance (*$P < 0.05$) compared with control. (D) Caspase3/7 activity in hemocytes of *P. vannamei* was detected when *P. vannamei* that successfully knocked down *Pv*LHPP was stimulated by *V. parahaemolyticus* for 4 h. Experiments were repeated at least three times and statistical difference between dsEGFP and ds*Pv*LHPP groups determined by Student's *t*-test. Asterisks indicate statistical significance (*$p<0.05$, ** $p< 0.01$). (E) The relative transcript level of Cytochrome C, P53, Caspase 3 and BAX in *P. vannamei* hemocyte were determined by qPCR in dsEGFP and ds*Pv*LHPP group.

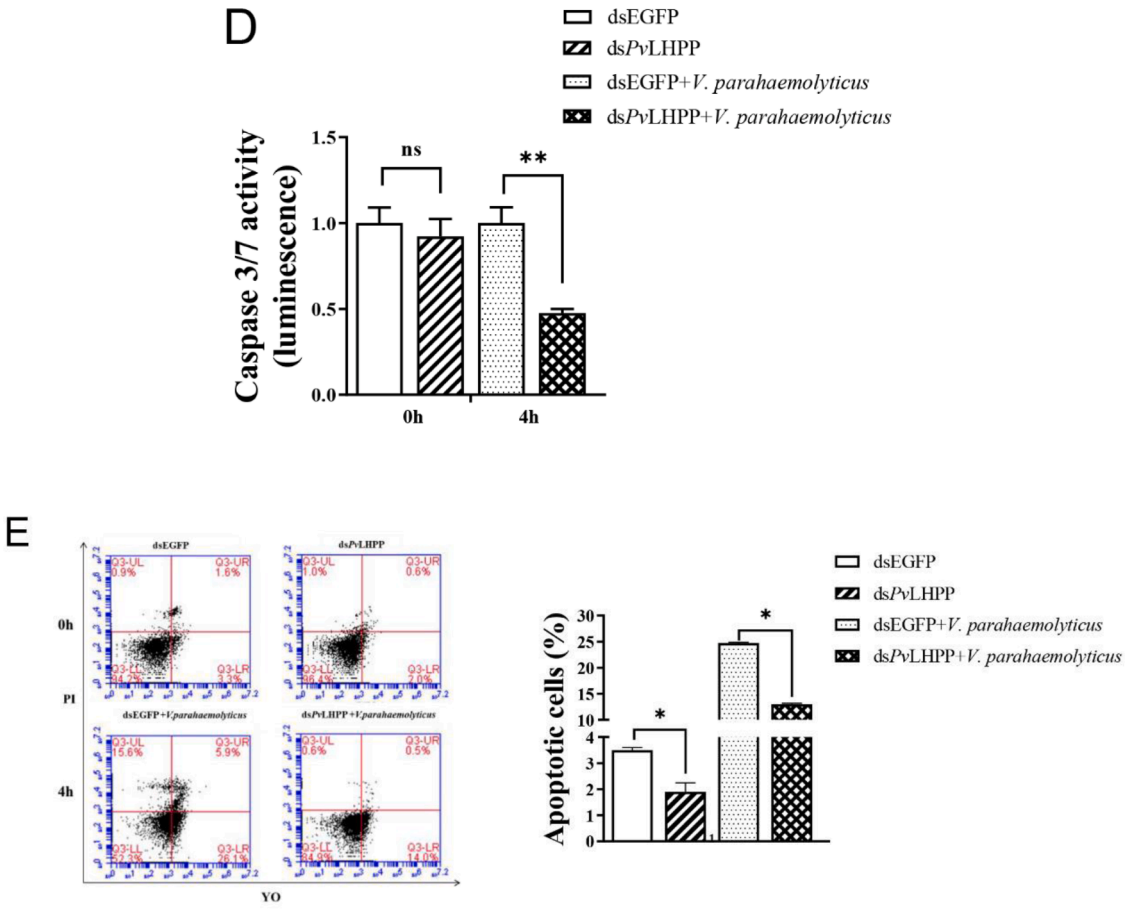

Fig. 4. (*continued*).

4. Discussion

Histidine phosphorylation (pHis) is a posttranslational modification associated with tumor cell fate that has recently been discovered in some mammals [18]. LHPP modulated histidine phosphorylation of protein is critically important in a variety of multi-cellular processes, including cell cycle, signal transduction, proliferation, differentiation and apoptosis, which estimated to account for 6% of all phosphorylated amino acids [19]. Here, we identified a novel LHPP homolog in *P. vannamei* (designated *Pv*LHPP). Sequence alignment and functional protein domain prediction revealed *Pv*LHPP was evolutionarily conserved in both invertebrate and vertebrate. The typical hydrolase 6 and hydrolase-like domain of *Pv*LHPP revealed that *Pv*LHPP is assigned to the haloacid dehydrogenase (HAD) superfamily of hydrolases [20], which determine the potential role of *Pv*LHPP in phosphoramidate hydrolase selective for pHis [21] and its related biological processes.

Emerging evidence has implicated LHPP as an important tumor suppressor [4,11,22,23], which participated in several apoptosis regulatory pathway. For instance, knockdown of *Pv*LHPP can significantly down-regulate active expression of Caspase 3 and poly ADP-ribose polymerase (PARP) in cervical cancer cells, while apoptotic of cancer cells also decreased significantly [11]. LHPP can promote pancreatic cancer (PaCa) cell apoptosis by increasing activation of cleaved-PARP and cleaved-Casp3 and reducing activation of cIAP1 [17]. Purpura can also up-regulate LHPP expression, thereby inducing transcriptional expression of apoptotic genes (Bax, Caspase-9 and Caspase-3) in HCT-116 cells [24]. Here, the role of *Pv*LHPP in the regulation of hemocytes apoptosis after *V. parahaemolyticus* challenge was elucidated, which demonstrated the evolutionarily conserved functions of LHPP in different species.

As a tumor suppressor, LHPP is normally expressed at low levels in tumor tissues and cells [25], similar in normal tissues, low expression of LHPP inhibited the cell renewal process [26]. In this study, the lowest expression of *Pv*LHPP in hemocyte and hepatopancreas have been confirmed, which might be beneficial to reduce the effect of pro-apoptotic response on the regeneration ability of these organs (Fig. 2), and implied that the rational allocation of LHPP expression in shrimp's immune system is a favorable immune balancing strategy for shrimp. Indeed, *Pv*LHPP presented a variety of responses under various pathogen stress in hemocyte and hepatopancreas, which indicated that LHPP was inducible in immune system (Fig. 3). Similarly, LHPP was selected as potential pathological marker in the gut of high-fat diet mice, which was negatively correlated with the abundance of *Candidatus_Saccharimonas* [27]. LPS stimulation also upregulated the expression of LHPP in *P. vannamei* [12]. These cumulative results suggest that *Pv*LHPP was an inducible factor that participated in innate immune response in *P. vannamei.*

In summary, an evolutionarily conserved LHPP from penaeid shrimp (*P. vannamei*) was characterized, and the pro-apoptotic effect of *Pv*LHPP on hemocyte apoptosis under *V. parahaemolyticus* was determined. Although the mechanism of *Pv*LHPP on apoptosis, and whether *Pv*LHPP participated in apoptosis is associated with mammalian in a conserved manner were still unknown. This study has been expected to provide new ideas for shrimp immune in the field of prevention and control of shrimp diseases.

Declaration of Competing Interest

The authors declared that they have no conflicts of interest to this work.

We declare that we do not have any commercial or associative

interest that represents a conflict of interest in connection with the work submitted.

Acknowledgments

This work was supported by National Natural Science Foundation of China (No. 32202976), China Postdoctoral Science Foundation (No. 2022M712013) and Shantou University Scientific Research Foundation for Talents (No. NTF20008).

References

[1] K.-H. Liu, A. Diener, Z. Lin, C. Liu, J. Sheen, Primary nitrate responses mediated by calcium signalling and diverse protein phosphorylation, J. Exp. Bot. 71 (15) (2020) 4428–4441.
[2] S.R. Fuhs, T. Hunter, pHisphorylation: the emergence of histidine phosphorylation as a reversible regulatory modification, Curr. Opin. Cell Biol. 45 (2017) 8–16.
[3] F. Yokoi, H. Hiraishi, K. Izuhara, Molecular cloning of a cDNA for the human phospholysine phosphohistidine inorganic pyrophosphate phosphatase, J. Biochem. 133 (5) (2003) 607–614.
[4] S.K. Hindupur, M. Colombi, S.R. Fuhs, M.S. Matter, Y. Guri, K. Adam, M. Cornu, S. Piscuoglio, C.K. Ng, C. Betz, The protein histidine phosphatase LHPP is a tumour suppressor, Nature 555 (7698) (2018) 678–682.
[5] L. Cui, F. Wang, Z. Yin, M. Chang, Y. Song, Y. Wei, J. Lv, Y. Zhang, Y. Tang, X. Gong, Effects of the LHPP gene polymorphism on the functional and structural changes of gray matter in major depressive disorder, Quant. Imaging Med. Surg. 10 (1) (2020) 257.
[6] N. Cai, T.B. Bigdeli, W. Kretzschmar, Y. Li, J. Liang, L. Song, J. Hu, Q. Li, W. Jin, Z. Hu, Sparse whole-genome sequencing identifies two loci for major depressive disorder, Nature 523 (7562) (2015) 588–591.
[7] R. Polimanti, Q. Wang, S.A. Meda, K.T. Patel, G.D. Pearlson, H. Zhao, L.A. Farrer, H.R. Kranzler, J. Gelernter, The interplay between risky sexual behaviors and alcohol dependence: genome-wide association and neuroimaging support for LHPP as a risk gene, Neuropsychopharmacology 42 (3) (2017) 598–605.
[8] D. Wang, Z. Ning, Z. Zhu, C. Zhang, Z. Meng, LHPP Suppresses Tumorigenesis of Intrahepatic Cholangiocarcinoma by Inhibiting the TGFβ/smad Signaling Pathway, Int. J. Biochem. Cell Biol. (2021), 105845.
[9] Y. Li, X. Zhang, X. Zhou, X. Zhang, LHPP suppresses bladder cancer cell proliferation and growth via inactivating AKT/p65 signaling pathway, Biosci. Rep. 39 (7) (2019).
[10] S. Liu, W. Gao, Y. Lu, Q. Zhou, R. Su, T. Hasegawa, J. Du, M. Li, As a novel tumor suppressor, LHPP promotes apoptosis by inhibiting the PI3K/AKT signaling pathway in oral squamous cell carcinoma, Int. J. Biol. Sci. 18 (2) (2022) 491.
[11] J. Zheng, X. Dai, H. Chen, C. Fang, J. Chen, L. Sun, Down-regulation of LHPP in cervical cancer influences cell proliferation, metastasis and apoptosis by modulating AKT, Biochem. Biophys. Res. Commun. 503 (2) (2018) 1108–1114.
[12] Y. Zhang, G. Gao, R. Lin, J.J. Aweya, M. Tao, F. Wang, Transcriptome analyses reveal Litopenaeus vannamei hemocytes response to lipopolysaccharide, Fish Shellfish Immunol. 76 (2018) 187–195.
[13] K.J. Livak, T.D. Schmittgen, Analysis of relative gene expression data using real-time quantitative PCR and the 2− ΔΔCT method, Methods 25 (4) (2001) 402–408.
[14] X. Xie, H. Li, L. Xu, F. Yang, A simple and efficient method for purification of intact white spot syndrome virus (WSSV) viral particles, Virus Res. 108 (1–2) (2005) 63–67.
[15] Q. Zhou, Y.-P. Qi, F. Yang, Application of spectrophotometry to evaluate the concentration of purified white spot syndrome virus, J. Virol. Method. 146 (1–2) (2007) 288–292.
[16] Q. Feng, Y. Huang, D. Yao, C. Zhu, S. Li, H. Ma, J.J. Aweya, Y. Zhang, Litopenaeus vannamei CK2 is involved in shrimp innate immunity by modulating hemocytes apoptosis, Fish Shellfish Immunol. 94 (2019) 643–653.
[17] F. Wu, Y. Chen, J. Zhu, LHPP suppresses proliferation, migration, and invasion and promotes apoptosis in pancreatic cancer, Biosci. Rep. 40 (3) (2020).
[18] H. Gong, Z. Fan, D. Yi, J. Chen, Z. Li, R. Guo, C. Wang, W. Fang, S. Liu, Histidine kinase NME1 and NME2 are involved in TGF-β1-induced HSC activation and CCl4-induced liver fibrosis, J. Mol. Histol. 51 (5) (2020) 573–581.
[19] J. Zhao, L. Zou, Y. Li, X. Liu, C. Zeng, C. Xu, B. Jiang, X. Guo, X. Song, HisPhosSite: a comprehensive database of histidine phosphorylated proteins and sites, J Proteom. 243 (2021), 104262.
[20] A.M. Burroughs, K.N. Allen, D. Dunaway-Mariano, L. Aravind, Evolutionary genomics of the HAD superfamily: understanding the structural adaptations and catalytic diversity in a superfamily of phosphoesterases and allied enzymes, J. Mol. Biol. 361 (5) (2006) 1003–1034.
[21] Y. Choi, S.H. Shin, H. Jung, O. Kwon, J.K. Seo, J.-M. Kee, Specific fluorescent probe for protein histidine phosphatase activity, ACS Sensor. 4 (4) (2019) 1055–1062.
[22] J. Li, H. Xie, Y. Ying, H. Chen, H. Yan, L. He, M. Xu, X. Xu, Z. Liang, B. Liu, YTHDF2 mediates the mRNA degradation of the tumor suppressors to induce AKT phosphorylation in N6-methyladenosine-dependent way in prostate cancer, Mol. Cancer 19 (1) (2020) 1–18.
[23] Q. Lin, J. Cai, Q.-Q. Wang, The significance of circular RNA DDX17 in prostate cancer, Biomed. Res. Int. 2020 (2020).
[24] Z. Li, X. Zhou, H. Zhu, X. Song, H. Gao, Z. Niu, J. Lu, Purpurin binding interacts with LHPP protein that inhibits PI3K/AKT phosphorylation and induces apoptosis in colon cancer cells HCT-116, J. Biochem. Mol. Toxicol. 35 (3) (2021) e22665.
[25] F. Wu, H. Ma, X. Wang, H. Wei, W. Zhang, Y. Zhang, The histidine phosphatase LHPP: an emerging player in cancer, Cell Cycle 21 (11) (2022) 1140–1152.
[26] R.M. Xia, D.B. Yao, X.M. Cai, X.Q. Xu, LHPP-mediated histidine dephosphorylation suppresses the self-renewal of mouse embryonic stem cells, Front. Cell Dev. Biol. 9 (2021), 638815.
[27] C. Guo, Y. Xu, X. Han, X. Liu, R. Xie, Z. Cheng, X. Fu, Transcriptomic and Proteomic Study on the High-Fat Diet Combined with AOM/DSS-Induced Adenomatous Polyps in Mice, Front. Oncol. (2021) 3369.